

Acoustic method for measurement of airtightness – field testing on three different existing office buildings in Germany

Björn Schiricke^{*1}, Benedikt Kölsch²

*1 German Aerospace Center (DLR),
Institute of Solar Research
Linder Höhe
51147 Cologne, Germany*

*2 German Aerospace Center (DLR),
Institute of Solar Research
Karl-Heinz-Beckurts-Str. 13,
52428 Jülich, Germany*

**Corresponding author: bjoern.schiricke@dlr.de*

ABSTRACT

Maintaining the airtightness of building envelopes is a key factor for the energy efficiency of buildings. A fast and reliable detection of leaks plays a decisive role, especially during building renovations. For this reason, work has been done in recent years to apply an acoustic beamforming method that enables the fast, simple, and large-area detection of leaks in building envelopes. This method is based on a microphone array technology and assumes that sound primarily follows the same paths as air through the building envelope. So far, these acoustic airtightness measurements have primarily been tested in the laboratory setting or on isolated facade parts with previously known leakages. Comprehensive field experience reports, particularly for use on a larger scale and on building envelopes with unknown leakages, have remained scarce.

This paper presents the results of large-scale testing and demonstration of acoustic air tightness measurements. Facades of 37 rooms of multi-storey buildings with unknown leakages were measured at three office buildings of different ages (built or renovated in 1990, 1995, and 2019) and heterogeneous building envelope structures. This represents, to the best of our knowledge, the most extensive field study to date for acoustic airtightness determination of building envelopes.

In the measurement campaign speakers emit white noise in the frequency range from 0.05 to 120 kHz from the inside with about 85 dB for a duration of four seconds. A microphone ring array with 48 microphones and a diameter of 0.75 m is located outside in a distance of up to 12 m from the observed facade. 57 measurements have been analysed and evaluated in a spectral range of 0.8 to 25 kHz.

As a result, hundreds of potential leaks were localized and visualized across a large area. Many of these were subsequently confirmed as plausible by visual inspection of the respective positions in the building envelope. Some were verified with a smoke stick test.

This paper introduces an Acoustic Assessment Score (ASS) for the evaluation of acoustic signals along with a colour code for their graphical representation. It enables a result representation that highlights the relevance of the signals concerning potential leakages. Furthermore, a Multi Frequency Assessment Score (MFAS) is defined, that allows a comparison of the acoustically determined airtightness of different rooms.

This field study has provided valuable experience into the practicality, speed, and interpretability of acoustic signals, along with the method's large-scale applicability and potential for further developments. The findings suggest, that a significant number of potential leakages can be detected, confirming the method's basic functionality for large buildings. Furthermore, a comparison of the distribution of the ASS and the MFAS within the different buildings suggests, that the applied acoustic method managed to discern the airtightness quality of the three buildings.

KEYWORDS

Airtightness, Beamforming, Leak detection, Building envelope, Field study

1 INTRODUCTION

The unintentional air exchange through a building envelope is estimated to account for 30 to 50 % of its heating and cooling energy. This unintentional airflow is a primary cause of heat loss in buildings, highlighting the need for effective airtightness measurements. Conventionally, the fan pressurization method (*ISO 9972:2015*, 2015) is used for this purpose. A fast and reliable detection of leaks plays a decisive role, especially in the renovation of buildings. However, identifying and quantifying leaks with standard methods in conjunction with a blower door test is challenging, time-consuming, and strongly depends on the experience of the respective energy consultant.

Recent advancements have seen the emergence of acoustic measurement methods, such as acoustic cameras, which hold the potential for identifying individual leaks in the building envelope. Unlike traditional methods, this non-destructive acoustic testing does not necessitate large volumes of air movement through the building envelope, allowing testing under naturally occurring unpressurized conditions. In contrast to the Blower-Door test, acoustic methods also do not rely on closed volume, enabling testing during the construction or renovation of a building.

In light of these advantages, there has been a focus on developing an acoustic beamforming method in recent years. Using an acoustic camera, this method enables the fast, simple, and large-area detection of potential leaks in building envelopes. This method is based on a microphone array technology, operating on the premise that sound primarily takes the same paths as air through the building envelope. In addition to other acoustic methods (Coltraco Ultrasonics, 2023), this presented method allows the detection of leaks on a large surface at once.

The aim of the acoustic measurements is to detect small openings in building enclosures and potential gas propagation pathways within buildings. A knowledge of leak location and estimates of leak sizes would enable a prioritized sealing of more substantial leaks (Walker & Wilson, 1998).

The objective of this work is to test and demonstrate the effectiveness of our acoustic air tightness measurement method on a larger scale. We applied this method to multi-storey buildings with unknown leakages and aimed to gain experience regarding the practicality, speed, and interpretability of the acoustic signals. Furthermore, we sought to assess the method's applicability method on a large scale, which has significant implications for its broader use.

2 TEST SITE AND MEASUREMENT CONFIGURATION

Within the framework of a project in which a heterogeneous building complex was also measured geometrically and thermally, the acoustic air tightness measurement was to be tested and demonstrated on a larger scale.

The test site selected for this study is a research institution consisting of five diverse buildings located in Villingen-Schwenningen, Germany. Figure 1 shows an aerial view and a 3D model of the investigated building complex. This measurement campaign focuses on office building parts A, D, and E, constructed or renovated approximately in 1990, 1995, and 2019. Building part B comprises clean rooms, and building part C houses a cogeneration unit. A total number

of 57 acoustic measurements have been analysed, corresponding to 36 investigated rooms (some of them had facades on different sides of the building so they required more than one measurement).

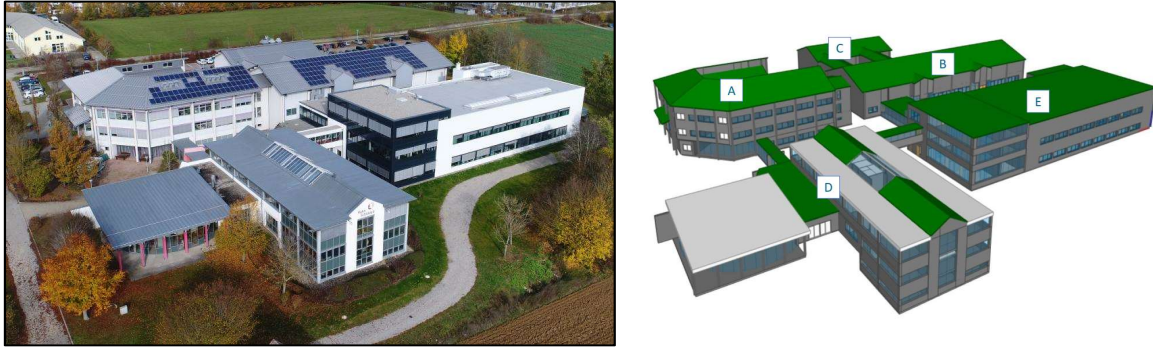


Figure 1: Aerial photo (left) and 3D-Model (right) of the investigated building complex, including labelling of the individual building parts

We used a microphone ring array with 48 uniformly spaced microphones with a diameter of 0.75 m for these measurements (see Figure 2, centre). This array functions optimally in a frequency range of 164 Hz to 20 kHz, although it can localize frequencies as high as 60 kHz. For this study, all signals were sampled at a frequency of 192 kHz and digitized with 32 bits. An optical camera positioned at the array's centre recorded a visual image of the measured scene, offering a resolution of 1920×1080 pixels.



Figure 2: Measurement setup: pair of loudspeakers inside (left), microphone array or acoustic camera outside (centre), visualization of the loudest noise sources on the facade (right).

In general, beamforming is a signal processing technique that enables the differentiation of sound sources from different directions using the microphone array. It operates by scanning a focus point \vec{x} on a pre-defined grid on the measured object. Equation 1 provides the time function $\hat{f}(\vec{x}, t)$ for this ring array for each focus point (Jaeckel, 2006):

$$\hat{f}(\vec{x}, t) = \frac{1}{M} \sum_{i=1}^M f_i(t - \Delta\tau_i) \quad (1)$$

During the evaluation, the individual microphones' time signals $f_i(t)$ are superimposed with a time delay $\Delta\tau_i$, corresponding to the time required for the sound wave to travel from the measured focus point on the building façade to the microphone. Subsequently, the time-corrected signals from all microphones are summed and divided by the total number of

microphones M , yielding a time signal for each focus point. Equation 2 is then used to calculate the effective sound pressure $\hat{p}_{rms}(\vec{x})$ at the calculated focus point:

$$\hat{p}_{rms}(\vec{x}) \approx \hat{p}_{rms}(\vec{x}, n) = \sqrt{\frac{1}{n} \sum_{k=0}^{n-1} \hat{f}^2(\vec{x}, t_k)} \quad (2)$$

where n is the total number of corresponding discrete time samples, and t_k is the time value at the sample index k . The advantage for various applications using an acoustic camera is the visual result, typically overlaid with a visible image of the same scene. For more information about the operating principle of the acoustic camera, see Refs. (Kölsch, 2022; Kölsch et al., 2021; Teutsch, 2007).

A pair of speakers (see Figure 2, left) is situated on one side of the wall (inside), while the acoustic camera (see Figure 2, centre) is placed on the other (outside). The high-frequency speaker functions in an even frequency range of 15 to 120 kHz, while the low-frequency dodecahedron speaker operates from 0.05 to 16 kHz. The stationary setup of the acoustic camera and speakers allowed for consistent measurements, with the sound waves penetrating through the leaks in the wall, detectable as individual sound sources on the wall's other side by the acoustic camera. A computer-generated white noise signal was emitted inside at a sound pressure level of 85 dB for 4 seconds.

The data analysis is carried out with the software NoiseImage (GFaI, 2021), specifically the power beamforming option, which enhances image clarity and source representation sharpness. While this method disrupts the exact sound pressure levels, it does not critically impact this application.

While we were able to reduce the disturbing influence of external sound sources in the past by recording reference signals next to the speaker inside the building (Kölsch et al., 2021), we did not do so in this study for efficiency and time-saving reasons.

3 METHODOLOGY OF CATEGORISATION

3.1 Evaluation of acoustic measurements

This measurement campaign has shown that sound sources indicating potential leakages, with the given equipment, are typically found within the spectral range of 800 Hz to 25 kHz. Within this range, there are 16 third-octave frequency bands. In each of these bands, only the highest Δ dB of the recorded sound pressure levels (hereafter referred to as sound peaks) are shown superimposed on the visual image. The Δ is chosen individually to provide optimal visualization for each case.

Since sound peaks can occur at different locations across different frequency bands, thereby indicating potential leakages at different locations, it is rarely possible to display all leakages simultaneously. Most of the time, a series of images across different frequency bands is needed to illustrate the potential leakages in the building envelope. This is exemplified in Figure 3 using Room 106 (Building D, east façade), where only eight of the 16 examined frequency bands are shown. Here, the highest 1.7 dB ($\Delta = 1.7$) sound peaks are displayed for all third-octave frequency bands. To comprehend the need for illustrating the entire range of frequency bands, we consider the peak in the third window from the left. It is only visible at the frequency bands 2, 6.3, and 10 kHz. Conversely, the leakage at the lower window frame in the second window from the right, is only visible at 2.5, 3.2, 4, 5, and 6.3 kHz.

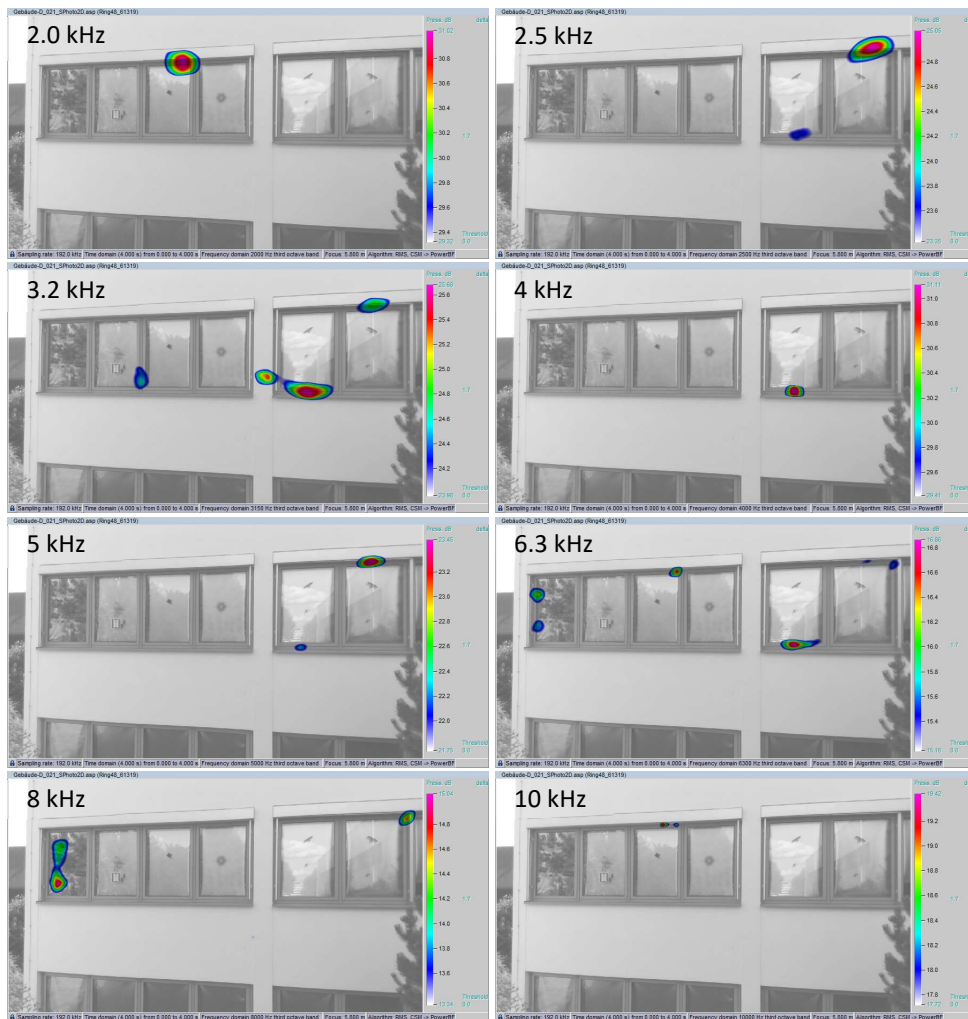


Figure 3: Representation of the results of the acoustic camera using the example of room 106 (building D, east facade). The highest 1.7 dB of the sound pressure level in each of the eight third-octave bands from 2 to 10 kHz are shown as coloured sound peaks. In the top left corner of each image, the average frequency of the third-octave band is noted.

Not every sound peak necessarily indicates a leakage; they can also result from sound reflections or structure-borne sound like vibrations, causing locally high sound levels. The sound peak on the pane of the left window in the 8 kHz example (Figure 3) is clearly located at an implausible place for leakage and is more likely caused by a vibration of the pane.

However, in many cases, a visual inspection at the locations of the sound peaks confirmed plausible causes for air leakage. An example is shown in Figure 4 (left), where a drilled hole from a previously installed window coincided with the position of the sound peak. In some rooms, a blower door and a smoke stick were employed, definitely confirming a leakage at the position of a sound peak (see Figure 4, right).

Often, however, the cause for a sound peak could not be clearly confirmed due to limited time resources. Therefore, these sound peaks required a subjective evaluation in terms of their plausibility for being leakage-related, which is further described in the following section.

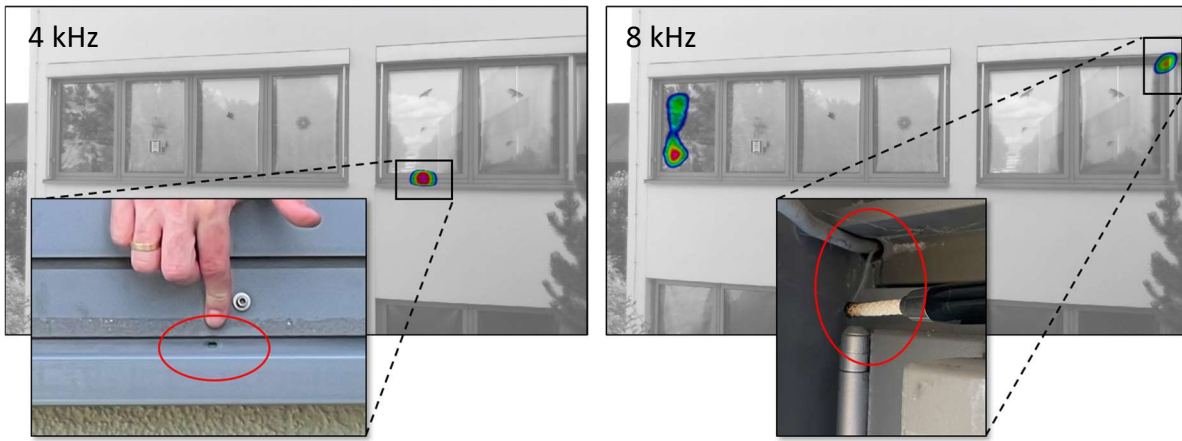


Figure 4: Examples of confirmed plausibility for air leakage as cause for sound peaks in room 106 (building D, east facade)

3.2 Categorization of the acoustic signals with regard to a possible leakage

The evaluation of individual peaks across all considered 16 third-octave frequency bands of all 57 measurements (in total 912 analysed frequency bands) required manual adjustment of the signal's peak Δ value in the software NoiseImage. This adjustment allowed the signal peak to be represented as the smallest possible area, thereby identifying the exact position of the source. The exact position of the peak is used to evaluate the plausibility of a leak being the cause of the sound source at that location. Table 1 describes the four evaluation categories with their colour code and scores.

Table 1: Description of the colour code for the evaluation of acoustic signals and their criteria

| Colour Code | Acoustic Assessment Score | Evaluation of acoustic signals | Description of subjective criteria |
|-------------|---------------------------|--------------------------------|--|
| ○ | 0 | very unlikely leakage | Peak of signal is at implausible location (e.g. on a window pane or facade panel, or outside the area under consideration) |
| ● | 1 | unlikely leakage | Some indications that the signal is probably not caused by a leakage (e.g. wide spread shape of the sound source) or Peak of signal is at rather implausible location (e.g. close to a plausible location but just off the mark) |
| ● | 2 | likely leakage | Peak of signal is at plausible location (e.g. joints between different materials or roof and wall), or even at particular plausible location, but with a much weaker signal. |
| ● | 3 | very likely leakage | Peak of signal is at a particular plausible location (e.g. seals in door and window frames) |

Identifying the exact location of the sound peak involves tedious manual work, and the assessment of the evaluation category is based on subjective criteria with fluid boundaries. Both tasks are time-consuming and susceptible to error, yet. Despite this, the method allows for documentation of the assessment in the facade representation using the corresponding colour code, as exemplified in Figure 5. Based on this representation, potential leakage locations on the facade can be identified for inspection and subsequent sealing if necessary. However, this process currently necessitates multiple images for the different third-octave frequency bands.

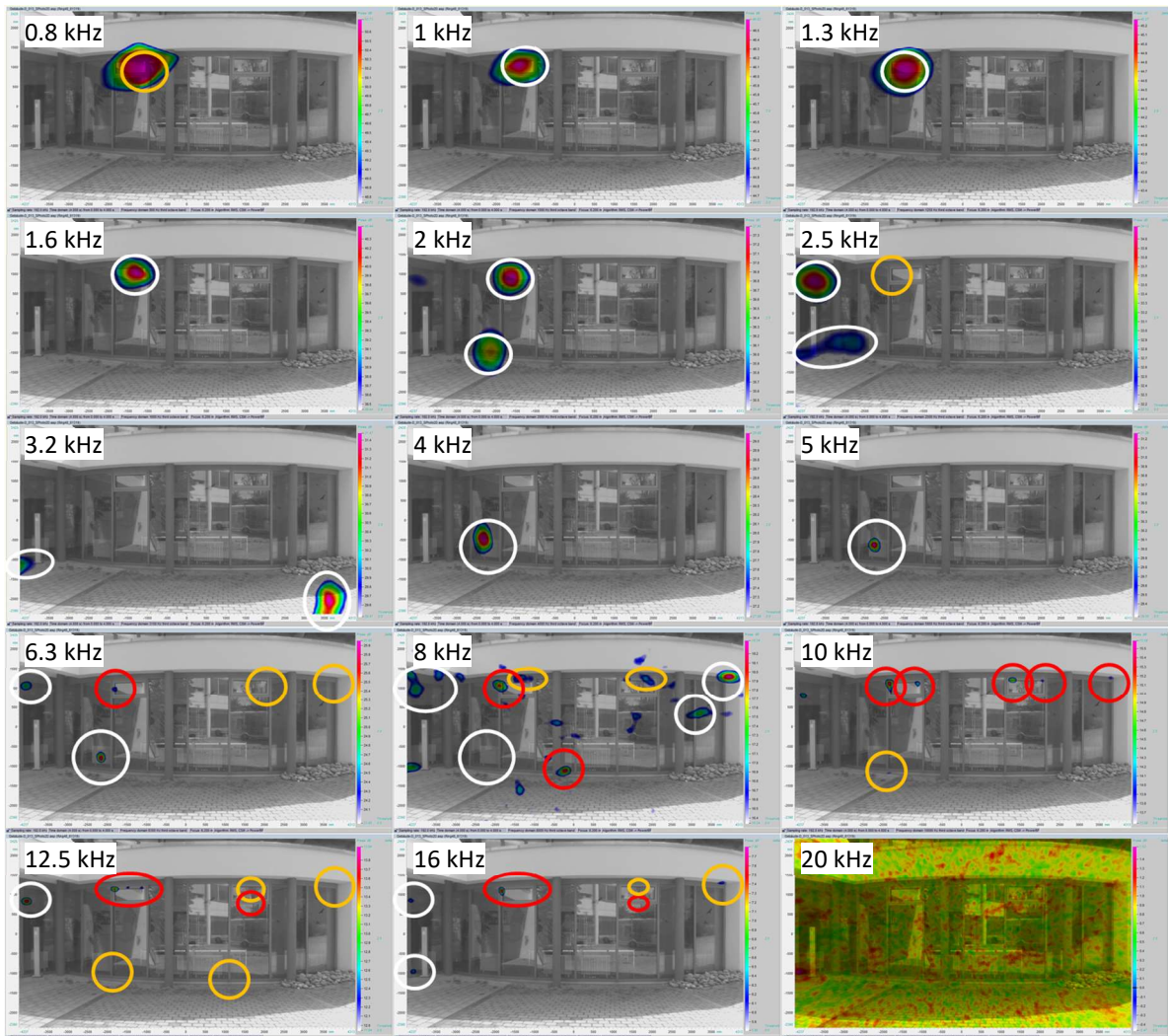


Figure 5: Representation of the evaluation of the sound peaks using the example of a corridor in building D with the colour codes of Table 1 for the third-octave bands from 0.8 to 20 kHz.

3.3 Evaluation of the airtightness of individual rooms on the facades

To summarise the evaluation of the airtightness of the individual rooms on the facades, the highest colour code assigned in the respective third-octave band is listed in a table (compare Table 2). This provides a visual summary indicating the frequency bands where signs of leakage were found.

As a quantitative metric for a certain room's airtightness, the so-called "multi frequency assessment score" is introduced. It is calculated as the sum of the "acoustic assessment scores" (see Table 1), corresponding to the highest colour codes assigned in each third-octave frequency band. This rules for calculation rule are admittedly arbitrary. We considered the possibility of weighting scores according to frequency range (e.g., giving less weight to lower frequency ranges), but we found no evidence to support this approach. Considering the number of sound peaks occurring for each third-octave band, instead of the score of the maximum occurring colour code, appeared to be less reproducible. Therefore, we opted for the simplest possible definition of the "multi frequency assessment score".

4 RESULTS AND DISCUSSION

Table 2 to Table 4 provide an overview of the evaluations for the building envelopes of the test site, representing all measured rooms/facades of buildings A, D, and E. The colour codes correspond to the “acoustic assessment score” (see Table 1), which are cumulatively represented in the “multi frequency assessment score”. In the second column, labelled “note”, we indicate the compass direction of the façade (if the room has more than one façade), or any special features of the measurement, such as detail shots or repetitions.

Table 2: Evaluation of acoustic signals for each measured room in Building D

| Room | | Third-octave frequency bands in kHz | | | | | | | | | | | | | | Multi Frequency Assessment Score | | | | |
|----------|----------|-------------------------------------|---|-----|-----|---|-----|-----|---|---|-----|---|----|------|----|----------------------------------|----|----|----|--|
| Name | note | 0.8 | 1 | 1.3 | 1.6 | 2 | 2.5 | 3.2 | 4 | 5 | 6.3 | 8 | 10 | 12.5 | 16 | 20 | 25 | | | |
| D-112 | S | ● | ● | ● | ● | ● | ○ | ○ | ○ | ○ | ○ | ○ | ○ | ○ | ○ | ○ | ○ | ○ | 12 | |
| | S up | ○ | ● | ● | ● | ● | ● | ● | ● | ● | ● | ● | ● | ● | ● | ● | ● | ● | 42 | |
| | SSW | ● | ○ | ○ | ○ | ○ | ○ | ○ | ○ | ○ | ○ | ○ | ○ | ○ | ○ | ○ | ○ | ○ | 15 | |
| | SW | ○ | ○ | ○ | ○ | ○ | ○ | ○ | ○ | ○ | ○ | ○ | ○ | ○ | ○ | ○ | ○ | ○ | 36 | |
| | SW | ○ | ○ | ○ | ○ | ○ | ○ | ○ | ○ | ○ | ○ | ○ | ○ | ○ | ○ | ○ | ○ | ○ | 39 | |
| | NW | ● | ● | ● | ● | ● | ● | ● | ● | ● | ● | ● | ● | ● | ○ | ○ | ○ | ○ | 28 | |
| D-112 | NW | ○ | ● | ○ | ● | ○ | ● | ○ | ● | ○ | ● | ○ | ● | ○ | ○ | ○ | ○ | 26 | | |
| Corridor | N | ● | ○ | ○ | ○ | ○ | ○ | ○ | ○ | ○ | ○ | ○ | ○ | ○ | ○ | ○ | ○ | 19 | | |
| | N detail | ○ | ○ | ○ | ○ | ○ | ○ | ○ | ○ | ○ | ○ | ○ | ○ | ○ | ○ | ○ | ○ | 27 | | |
| D-109 | | ○ | ○ | ○ | ○ | ○ | ○ | ○ | ○ | ○ | ○ | ○ | ○ | ○ | ○ | ○ | ○ | 24 | | |
| D-108 | W | ○ | ● | ● | ● | ● | ● | ● | ● | ● | ● | ● | ● | ○ | ○ | ○ | ○ | 31 | | |
| | S | ○ | ○ | ○ | ○ | ○ | ○ | ○ | ○ | ○ | ○ | ○ | ○ | ○ | ○ | ○ | ○ | 35 | | |
| D-107 | | ○ | ○ | ○ | ○ | ○ | ○ | ○ | ○ | ○ | ○ | ○ | ○ | ○ | ○ | ○ | ○ | 36 | | |
| D-106 | S | ○ | ○ | ○ | ○ | ○ | ○ | ○ | ○ | ○ | ○ | ○ | ○ | ○ | ○ | ○ | ○ | 36 | | |
| | E | ○ | ○ | ○ | ○ | ○ | ○ | ○ | ○ | ○ | ○ | ○ | ○ | ○ | ○ | ○ | ○ | 36 | | |
| D-103 | | ○ | ○ | ○ | ○ | ○ | ○ | ○ | ○ | ○ | ○ | ○ | ○ | ○ | ○ | ○ | ○ | 19 | | |
| D-211 | | ○ | ○ | ○ | ○ | ○ | ○ | ○ | ○ | ○ | ○ | ○ | ○ | ○ | ○ | ○ | ○ | 29 | | |
| D-210 | | ○ | ○ | ○ | ○ | ○ | ○ | ○ | ○ | ○ | ○ | ○ | ○ | ○ | ○ | ○ | ○ | 18 | | |
| D-209 | | ○ | ○ | ○ | ○ | ○ | ○ | ○ | ○ | ○ | ○ | ○ | ○ | ○ | ○ | ○ | ○ | 33 | | |
| D-208 | W | ○ | ○ | ○ | ○ | ○ | ○ | ○ | ○ | ○ | ○ | ○ | ○ | ○ | ○ | ○ | ○ | 29 | | |
| | S | ○ | ○ | ○ | ○ | ○ | ○ | ○ | ○ | ○ | ○ | ○ | ○ | ○ | ○ | ○ | ○ | 37 | | |
| D-207 | | ○ | ○ | ○ | ○ | ○ | ○ | ○ | ○ | ○ | ○ | ○ | ○ | ○ | ○ | ○ | ○ | 33 | | |
| D-206 | S | ○ | ○ | ○ | ○ | ○ | ○ | ○ | ○ | ○ | ○ | ○ | ○ | ○ | ○ | ○ | ○ | 33 | | |
| | E | ○ | ○ | ○ | ○ | ○ | ○ | ○ | ○ | ○ | ○ | ○ | ○ | ○ | ○ | ○ | ○ | 38 | | |
| D-205 | | ○ | ○ | ○ | ○ | ○ | ○ | ○ | ○ | ○ | ○ | ○ | ○ | ○ | ○ | ○ | ○ | 29 | | |
| D-204 | | ○ | ○ | ○ | ○ | ○ | ○ | ○ | ○ | ○ | ○ | ○ | ○ | ○ | ○ | ○ | ○ | 19 | | |
| D-203 | | ○ | ○ | ○ | ○ | ○ | ○ | ○ | ○ | ○ | ○ | ○ | ○ | ○ | ○ | ○ | ○ | 29 | | |
| D-202 | | ○ | ○ | ○ | ○ | ○ | ○ | ○ | ○ | ○ | ○ | ○ | ○ | ○ | ○ | ○ | ○ | 37 | | |
| D-201 | | ○ | ○ | ○ | ○ | ○ | ○ | ○ | ○ | ○ | ○ | ○ | ○ | ○ | ○ | ○ | ○ | 23 | | |
| Bridge | S | ○ | ○ | ○ | ○ | ○ | ○ | ○ | ○ | ○ | ○ | ○ | ○ | ○ | ○ | ○ | ○ | 19 | | |
| | N | ○ | ○ | ○ | ○ | ○ | ○ | ○ | ○ | ○ | ○ | ○ | ○ | ○ | ○ | ○ | ○ | 18 | | |
| | N detail | ○ | ○ | ○ | ○ | ○ | ○ | ○ | ○ | ○ | ○ | ○ | ○ | ○ | ○ | ○ | ○ | 21 | | |

Table 3: Evaluation of acoustic signals for each measured room in Building E

| Room | | Third-octave frequency bands in kHz | | | | | | | | | | | | | | Multi Frequency Assessment Score | | | |
|------------|--------------|-------------------------------------|---|-----|-----|---|-----|-----|---|---|-----|---|----|------|----|----------------------------------|----|----|--|
| Name | note | 0.8 | 1 | 1.3 | 1.6 | 2 | 2.5 | 3.2 | 4 | 5 | 6.3 | 8 | 10 | 12.5 | 16 | 20 | 25 | | |
| E-Büro 2 | 2.floor (OG) | ○ | ○ | ○ | ○ | ○ | ○ | ○ | ○ | ○ | ○ | ○ | ○ | ○ | ○ | ○ | ○ | 14 | |
| E-Büro 1 | 2.floor (OG) | ○ | ○ | ○ | ○ | ○ | ○ | ○ | ○ | ○ | ○ | ○ | ○ | ○ | ○ | ○ | ○ | 20 | |
| E-Büro | 2.floor (EG) | ○ | ○ | ○ | ○ | ○ | ○ | ○ | ○ | ○ | ○ | ○ | ○ | ○ | ○ | ○ | ○ | 5 | |
| E-Büro | | ○ | ○ | ○ | ○ | ○ | ○ | ○ | ○ | ○ | ○ | ○ | ○ | ○ | ○ | ○ | ○ | 8 | |
| E-Bespr. | | ○ | ○ | ○ | ○ | ○ | ○ | ○ | ○ | ○ | ○ | ○ | ○ | ○ | ○ | ○ | ○ | 9 | |
| E-Bespr. 2 | 1.floor (UG) | ○ | ○ | ○ | ○ | ○ | ○ | ○ | ○ | ○ | ○ | ○ | ○ | ○ | ○ | ○ | ○ | 21 | |
| E-Büro 1 | | ○ | ○ | ○ | ○ | ○ | ○ | ○ | ○ | ○ | ○ | ○ | ○ | ○ | ○ | ○ | ○ | 15 | |
| E-Büro | | ○ | ○ | ○ | ○ | ○ | ○ | ○ | ○ | ○ | ○ | ○ | ○ | ○ | ○ | ○ | ○ | 24 | |
| E-Aufenth. | 2.floor (EG) | ○ | ○ | ○ | ○ | ○ | ○ | ○ | ○ | ○ | ○ | ○ | ○ | ○ | ○ | ○ | ○ | 10 | |
| E-Büro | 1.floor (UG) | ○ | ○ | ○ | ○ | ○ | ○ | ○ | ○ | ○ | ○ | ○ | ○ | ○ | ○ | ○ | ○ | 13 | |

Table 4: Evaluation of acoustic signals for each measured room in Building A

| Room | | Third-octave frequency bands in kHz | | | | | | | | | | | | | | | Multi Frequency Assessment Score | | |
|---------|-----------------|-------------------------------------|---|-----|-----|---|-----|-----|---|---|-----|---|----|------|----|----|----------------------------------|----|--|
| Name | note | 0.8 | 1 | 1.3 | 1.6 | 2 | 2.5 | 3.2 | 4 | 5 | 6.3 | 8 | 10 | 12.5 | 16 | 20 | 25 | | |
| A-101 | SW | ● | ● | ● | ○ | ○ | ○ | ○ | ○ | ○ | ○ | ○ | ○ | ○ | ○ | ○ | ○ | 12 | |
| | SW - detail | ● | ● | ● | ○ | ● | ● | ● | ● | ● | ○ | ○ | ○ | ○ | ○ | ○ | ○ | 26 | |
| | NW | ● | ● | ● | ○ | ○ | ● | ● | ● | ● | ○ | ○ | ○ | ○ | ○ | ○ | ○ | 27 | |
| | NW | ○ | ○ | ○ | ○ | ○ | ○ | ○ | ○ | ○ | ○ | ○ | ○ | ○ | ○ | ○ | ○ | 9 | |
| A-103 | | ○ | ○ | ○ | ○ | ○ | ○ | ○ | ○ | ○ | ○ | ○ | ○ | ○ | ○ | ○ | 16 | | |
| A-201/1 | | ○ | ○ | ○ | ○ | ○ | ○ | ○ | ○ | ○ | ○ | ○ | ○ | ○ | ○ | ○ | 3 | | |
| | detail | ● | ● | ○ | ○ | ○ | ○ | ○ | ○ | ○ | ○ | ○ | ○ | ○ | ○ | ○ | 13 | | |
| A-201/2 | | ○ | ○ | ○ | ○ | ○ | ○ | ○ | ○ | ○ | ○ | ○ | ○ | ○ | ○ | ○ | 13 | | |
| A-201/3 | | ○ | ○ | ○ | ○ | ○ | ○ | ○ | ○ | ○ | ○ | ○ | ○ | ○ | ○ | ○ | 15 | | |
| A-202 | NW | ○ | ○ | ○ | ○ | ○ | ○ | ○ | ○ | ○ | ○ | ○ | ○ | ○ | ○ | ○ | ○ | 16 | |
| | Diagrammbereich | ○ | ○ | ○ | ○ | ○ | ○ | ○ | ○ | ○ | ○ | ○ | ○ | ○ | ○ | ○ | ○ | 16 | |
| | SW rep. 1 | ○ | ○ | ○ | ○ | ○ | ○ | ○ | ○ | ○ | ○ | ○ | ○ | ○ | ○ | ○ | ○ | 19 | |
| | SW rep. 2 | ○ | ○ | ○ | ○ | ○ | ○ | ○ | ○ | ○ | ○ | ○ | ○ | ○ | ○ | ○ | ○ | 12 | |
| | SW rep. 3 | ○ | ○ | ○ | ○ | ○ | ○ | ○ | ○ | ○ | ○ | ○ | ○ | ○ | ○ | ○ | ○ | 11 | |
| A-102 | | ○ | ○ | ○ | ○ | ○ | ○ | ○ | ○ | ○ | ○ | ○ | ○ | ○ | ○ | ○ | 8 | | |

This overview can be used to assess if the applied acoustic method managed to discern any differences among the different buildings. This is reflected both visually in the distribution of the colour codes in Table 2 to Table 4 as well as in the frequency distribution shown in Table 5. As expected, Building D, which is the oldest building and was already identified as problematic by the building owner, exhibits the highest values in the "multi frequency assessment score". A high score indicates a strong acoustic evidence of leakage and, thus, a poor air tightness rating. Table 5 presents the frequency distribution of this numerical assessment of facades.

Table 5: Overall assessment of the acoustic leakage analyses for the three Buildings

| Acoustic Multi Frequency Assessment Score | Number of measurements with that score per building | | |
|---|---|----------|----------|
| | D (1990) | A (1995) | E (2019) |
| very low (0-9) | 0 | 3 | 3 |
| low (10-19) | 8 | 10 | 4 |
| mid (20-29) | 10 | 2 | 3 |
| high (30-39) | 13 | 0 | 0 |
| very high (40-48) | 1 | 0 | 0 |
| total number of meas. | 32 | 15 | 10 |

5 CONCLUSIONS

This measurement campaign, to our knowledge, represents the most extensive field study conducted to date on the acoustic determination of airtightness of building envelopes. The method was successfully demonstrated on facades of multi-storey buildings of different ages and heterogeneous building envelope structures. Potential leaks were localized and visualized across large areas, with many of them confirmed as plausible by visual inspection. In selected rooms where smoke sticks were employed, some identified leakages were verified. In comparison to the well established infrared thermography method for visualizing leaks, this acoustic method does not rely on temperature or pressure differences across the building envelope.

This field study yields valuable insights regarding the practicability, speed, and interpretability of the acoustic signals and the broader applicability of the method. The findings suggest that a significant number of potential leakages can be detected, confirming the method's basic functionality for large buildings.

However, despite these advancements, further research is needed, particularly in interpreting the data. Possible developments include greater automation in the assessment of relevant leakage locations. This implies the need for systematic laboratory or field investigation with known leakages. Factors like wind influence or reflection of other outside sound sources on the shifting of acoustic peaks and the interpretation of results should also be accounted for.

Moving forward, we envision further detailed examinations at testing facilities and renovation sites. Enhancements to the measurement technology are also projected, such as combining infrared thermography with the existing acoustic camera setup to improve leak detection reliability. The development of a suitable ultrasonic transmitter is another area for exploration.

The potential of this methodology is significant. Noise reduction through reference signals (like done in (Kölsch et al., 2021)), the use of acoustic spectra to infer the type and size of leaks, and multi-perspective analysis to rule out reflections are promising future developments. Furthermore, visualizing leaks from various third-octave frequency bands in a single image could improve the leak-finding process.

6 ACKNOWLEDGEMENTS

This work is part of the research project “Pilotanwendung von Gebäudetomograph-Messmethoden an einem Institut der Innovationsallianz Baden-Württemberg (Gtom-innBW)” which was funded by the Ministry of Economic Affairs, Labour and Tourism Baden-Württemberg under the grant number: WM3-4332-157/64. The authors thank the “Hahn-Schickard-Gesellschaft für angewandte Forschung e.V.” in Villingen-Schwenningen for providing their office buildings as test cases. Additionally, the authors thank Dirk Döbler, Dr. Olaf Jaeckel and Dr. Fabian Knappe from “GFaI - Gesellschaft zur Förderung angewandter Informatik e.V.” for fruitful discussions regarding these measurement results.

7 REFERENCES

- Coltraco Ultrasonics. (2023). *Ultrasonic Airtightness, Leak Detection and Quantification System*. <https://coltraco.com/coltraco-products/portascanner-airtight/>
- GFaI. (2021). *Software: NoiseImage* (4.13.4.17964).
- ISO 9972:2015—*Thermal performance of buildings - Determination of air permeability of buildings - Fan pressurization method* (9972:2015). (2015).
- Jaeckel, O. (2006). Strengths and weaknesses of calculating beamforming in the time domain. *Proceedings of the 8th Berlin Beamforming Conference*.
- Kölsch, B. (2022). *Investigation of an improved acoustical method for determining airtightness of building envelopes* [Dissertation]. RWTH Aachen University.
- Kölsch, B., Schiricke, B., Lüpfert, E., & Hoffschmidt, B. (2021). Detection of air leakage in building envelopes using microphone arrays. *Proceedings of the 41st AIVC - ASHRAE IAQ Joint Conference*.
- Teutsch, H. (2007). *Modal array signal processing: Principles and applications of acoustic wavefield decomposition*. Springer.
- Walker, I. S., & Wilson, D. J. (1998). Field Validation of Algebraic Equations for Stack and Wind Driven Air Infiltration Calculations. *HVAV&R Research*, 1(2).